Fracture behaviors of bulk metallic glasses under complex tensile loading

Li Yu[1], Tzu-Chiang Wang[2*]

State Key Laboratory of Nonlinear Mechanics, Institute of Mechanics, Chinese Academy of Sciences.

Beijing 100190, China

Correspondence and requests for materials should be addressed to: Tzu-Chiang Wang (email: tcwang@imech.ac.cn)

Abstract: Up to now the theoretical analysis for fracture behaviors of bulk metallic glasses (BMGs) are limited to uniaxial loading. However, materials usually suffer complex stress conditions in engineering applications. Thus, to establish an analysis method that could describe fracture behaviors of BMGs under complex loading is rather important. In this paper, a universal formula for the fracture angle is proposed towards solving this problem. The ellipse criterion is used as an example to show how to predict fracture behaviors of BMGs subjected to complex loading according to this formula. In this case, both the fracture strength and fracture angle are found to be well consistent with experimental data.

Key words: Fracture behaviors; complex loading; bulk metallic glasses; ellipse criterion; fracture angle;

1. Introduction

Metallic glasses represent a relative young class of materials, which have been first discovered in 1960 by performing classic rapid-quenching experiments on Au-Si alloys[1]. Until now, the formation, structure and properties of bulk metallic glasses (BMGs) have been extensively explored over half a century [2-4]. In particular, its mechanical behaviors and properties arouse great fundamental scientific interests. For

example, the absence of cry-slip mechanisms in BMGs leads to its ultra high strength that is close to the theoretical limit[3], and also the normal stress sensitive mechanical responses give rise to the tension-compression asymmetry, that is, uniaxial tension and compression in BMGs represent distinct fracture behaviors. Despite the negligible ductility under uniaxial stretching and lack of strain hardening during compression [5-10], the striking mechanical attributes help BGMs stand out of various metallic materials.

A lot of efforts are dedicated to investigate the facture behavior of BMGs [11-13]. Based on these studies, a general conclusion could be drawn: for most BMGs, the compressive strength is higher than the tensile one, and their fracture planes deviate from the maximum resolved shear stress plane (45°). To be specific, the fracture angle is slightly smaller than 45° under compression, while this angle becomes markedly larger than 45° when the BGMs sample is subject to uniaxial tension. It suggests that normal stress plays an important role in fracture behaviors of BMGs and leads to the tension-compression asymmetry mentioned above. This point of view is further supported by recent studies, where the axial fracture strength and angle are found to be associated with the confining pressure [13-16].

Due to the tension-compression asymmetry, classical fracture criteria fail to provide even a qualitative description to fracture behaviors of BMGs, since the influence of normal stress is not considered. To overcome this problem, several fracture criteria are proposed for BMGs, for example, the Mohr-Coulomb (M-C) criterion [17, 18] and ellipse criterion[19] are suggested to describe the normal stress effect on BMGs. Up to now, the existing studies of experiment and theory based on these fracture criteria are limited to simple uniaxial loading. However, materials usually suffer complex stress conditions in engineering applications. Thus, to establish an analysis method that could predict fracture behaviors of BMGs under complex loading is rather important.

In this paper, we establish a universal formula for the fracture angle towards

analyzing fracture behaviors of BMGs under complex loading. To the best of our knowledge, this is the first time that fracture behaviors of BMGs under complex loading is explicitly discussed. The ellipse criterion is used as an example to show how to apply our formula to a specific case. In this case, fracture behaviors of BMGs depends on loading modes, and the corresponding variation of the fracture strength and angle for BMGs under complex loading is carefully studied. Through comparing theoretical analysis results with existing experiments for complex loading, we find that our theoretical analysis method can well predict fracture behaviors of $Zr_{41}Ti_{14}Cu_{12.5}Ni_{10}Be_{22.5}$. Furthermore, we establish a sister ellipse fracture criterion based on the maximum shear stress and average stress, which should be more convenient for engineering applications.

2. The basic formula and its applications

2.1 The basic formula

Fracture criteria are used to predict the fracture of materials. Usually, normal stress (σ) and shear stress (τ) on the fracture plane are used as basic variables in fracture criteria, such as the M-C criterion, maximum shear stress criterion and ellipse criterion. Thus, its general form can be expressed as

$$f(\sigma,\tau)=0. \tag{1}$$

Furthermore, when materials are under complex loading, the fracture plane is located at the plane of first principal stress σ_I and third principal stress σ_{III}. Thus, the shear and normal stress on the fracture plane can be expressed as

$$\sigma=\sigma_M-\tau_M\cos(2\theta_T), \tag{2}$$

and

$$\tau=\tau_M\sin(2\theta_T), \tag{3}$$

where mean stress $\sigma_M=(\sigma_I+\sigma_{III})/2$, maximum shear stress $\tau_M=(\sigma_I-\sigma_{III})/2$, and θ_T is the tensile fracture angle between the fracture plane and axis of the first

principal stress. By using Eqs.(2)-(3), Eq. (1) can be re-expressed as a function of θ_T, and the most dangerous plane can be found by seeking the extreme point of this function.

$$\frac{\partial f}{\partial \sigma}\frac{d\sigma}{d\theta}+\frac{\partial f}{\partial \tau}\frac{d\tau}{d\theta}=0, \tag{4}$$

Based on Eqs.(2)-(4), the fracture angle can be expressed as

$$tg\left(2\theta_T\right)=-\frac{\partial f/\partial \tau}{\partial f/\partial \sigma}. \tag{5}$$

The fracture strength and angle for different loading modes can be obtained from Eqs.(2), (3) and (5). Note that the formula (5) for the fracture angle of BMGs under complex loading is not limited to specific fracture criteria. Hence, it is a universal formula even could be applied to analyze fracture behaviors of other materials.

2.2 Applying the universal formula to a specific case

In the following, the ellipse criterion will be used as an example to analyze fracture behaviors of BMGs under complex loading. The ellipse criterion can be written as[19]

$$\tau^2+\alpha^2\sigma^2=\tau_0^2, \tag{6}$$

where $\alpha=\tau_0/\sigma_0$ is a parameter to reflect the effect of the normal stress. Note that τ_0 is the critical shear fracture stress and σ_0 is the critical normal fracture stress on the fracture plane.

Journal of Applied Mechanics. Received August 28, 2017;
Accepted manuscript posted October 30, 2017. doi:10.1115/1.4038286

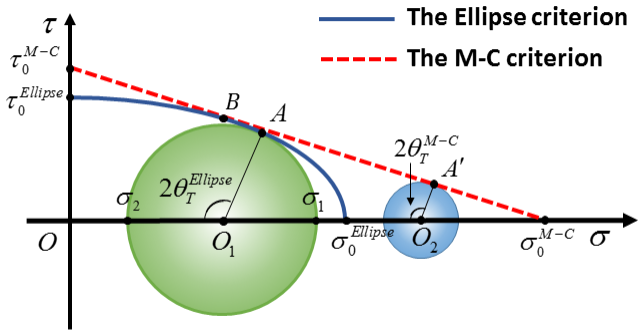

Fig. 1. Illustration of the critical fracture lines and critical Mohr circle of the M-C criterion and ellipse criterion in the case of tensile loading. The ellipse is tangent to the straight line at point B according to the uniaxial tensile experimental data. The τ_0^{M-C}, $\tau_0^{Ellipse}$, σ_0^{M-C}, $\sigma_0^{Ellipse}$, θ_T^{M-C} and $\theta_T^{Ellipse}$ in the plot denote the critical shear fracture stresses, critical fracture normal stresses and fracture angles predicted by the M-C criterion and ellipse criterion, respectively.

The critical fracture lines of ellipse criterion in σ-τ coordinate system are shown in Fig. 1, where the M-C criterion is also shown to compare with the ellipse criterion. With complex loading, the critical Mohr circles of two criteria could be plotted (see Fig. 1), and it could be seen that the critical points shown in Eq. (5) correspond to the tangent points between the critical Mohr circles and fracture lines. Thus, the fracture strength and angle of the ellipse criterion (M-C criterion) can be obtained from the tangent point A (A′).

It is obvious that the fracture angle predicted by M-C criterion remains unchanged under different loading. However, the pure shear experiment[21] shows that the fracture in BMGs occurs along the pure shear plane (corresponding to a fracture angle of 45°), which is quite different from its uniaxial tensile fracture angle (markedly larger than 45°). This variation of fracture angles for different loading modes cannot be captured by the M-C criterion, while it could be well described with the ellipse criterion.

Journal of Applied Mechanics. Received August 28, 2017;
Accepted manuscript posted October 30, 2017. doi:10.1115/1.4038286

To compare with the experimental results, we consider BMGs under axial loading in x_1- axis and confining loading shown in Fig. 2(a).

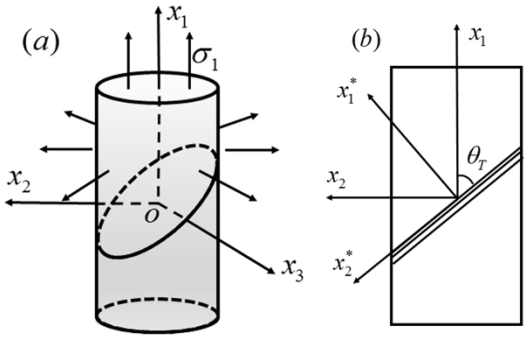

Fig. 2. The stress state and shear plane of cylindrical specimen. (a) The stress state and shear plane are shown. (b) The shear plane and fracture angle are shown in the x_1-x_2 plane.

The confining pressure is proportional to the axial loading

$$\sigma_{22}=\sigma_{33}=\rho\sigma_{11}\left(-1<\rho<1,\ \sigma_{11}>0\right), \tag{7}$$

where σ_{ii} are the normal stress in the x_i- axis, and ρ is the proportionality coefficient between the axial stress and confining pressure. Since the stress state of the cylindrical specimen is symmetric with respect to the x_1- axis, we can consider the normal of the fracture plane locates at the x_1-x_2 plane as shown in Fig.2 (b). Thus, the stress states can be characterized by σ_{11} and σ_{22}, based on which the mean stress and maximum shear stress can be expressed as

$$\sigma_M=\left(1+\rho\right)\sigma_{11}/2, \tag{8}$$

and

$$\tau_M=\left(1-\rho\right)\sigma_{11}/2=\chi\left(\rho\right)\sigma_M, \tag{9}$$

where $\chi\left(\rho\right)=(1-\rho)/\left(1+\rho\right)$ is a function of the proportionality coefficient ρ. Then, by substituting the equation of the ellipse criterion into Eq. (5), the dependence

between the fracture stress and fracture angle can be obtained,

$$\frac{\tau}{\alpha^2\sigma} = -tg\left(2\theta_T\right). \tag{10}$$

Moreover, the stress state on the fracture plane can be expressed as,

$$\sigma = \sigma_M - \tau_M \cos\left(2\theta_T\right) = \left[1 - \chi\cos\left(2\theta_T\right)\right]\sigma_M, \tag{11}$$

and

$$\tau = \tau_M \sin\left(2\theta_T\right) = \chi\sigma_M \sin\left(2\theta_T\right). \tag{12}$$

By combining Eq. (10), Eq. (11) and Eq. (12), the dependence of the fracture angle θ_T on the proportionality coefficient could be given:

$$\cos\left(2\theta_T\right) = -\frac{1}{\chi(\rho)}\frac{\alpha^2}{1-\alpha^2}. \tag{13}$$

Eq.(13) indicates that the fracture angle changes with different loading modes. This result could be used to explain the loading mode dependent fracture behaviors in BMGs. Substituting Eq. (10) into the Eqs. (2) and (3) leads to

$$\alpha\ \sigma = -\tau_0 \cos\left(2\theta_T\right)/\sqrt{a}, \tag{14}$$

for $\sigma > 0$, and

$$\tau = \alpha\tau_0 \sin\left(2\theta_T\right)/\sqrt{a}, \tag{15}$$

where

$$a = \cos^2\left(2\theta_T\right) + \alpha^2 \sin^2\left(2\theta_T\right). \tag{16}$$

By Substituting Eqs. (14) and (15) into Eqs. (11) and (12), τ_M and σ_M could be written as

$$\tau_M = \alpha\tau_0/\sqrt{a}, \tag{17}$$

and

$$\alpha\sigma_M = -\tau_0 \cos\left(2\theta_T\right)\left(1-\alpha^2\right)/\sqrt{a}. \tag{18}$$

Finally, Eq. (17) and Eq. (18) are combined to obtain the following formula,

$$\tau_M^2 + \beta^2\sigma_M^2 = \tau_0^2, \tag{19}$$

where $\beta^2 = \alpha^2/(1-\alpha^2)$. Eq. (19) shows that the relation between σ_M and τ_M is similar to the Eq. (6). Thus, the Eq. (19) presents a new ellipse criterion based on the mean stress σ_M and maximum shear stress τ_M, which should be more convenient for engineering applications. This is because the mean stress σ_M and maximum shear stress τ_M are directly related to external loads, while the normal stress σ and shear stress τ can only be obtained after the fracture angle is determined.

Fracture behaviors of BMGs under complex loading can described by Eqs.(13)-(15). Once the parameters α, τ_0 of the ellipse criterion and proportionality coefficient ρ are given, the fracture angle and strength could be obtained.

3. Results and discussion

From the Eq. (13), we can find that ρ can only change within a certain range by considering $\cos(2\theta_T)$ takes the values from -1 to 1. In the case of $\cos(2\theta_T) = -1$, ρ can be solved by Eq. (13), which is

$$\rho_{cr} = 1 - 2\alpha^2. \tag{20}$$

Note that Eq. (20) shows that ρ is less than $\rho_{cr} = 1-2\alpha^2$, and we first analyze fracture behaviors of BMGs in the case $-1 \le \rho \le \rho_{cr}$.

3.1 Fracture behaviors of bulk metallic glasses in the case $-1 \le \rho \le \rho_{cr}$

Let us consider $Zr_{52.5}Cu_{17.9}Ni_{14.6}Al_{10}Ti_5$ BMGs, in this system $\theta_T = 50.7^\circ$ and $\sigma_T = 1660\,\text{Mpa}$ for uniaxial tension[22]. The corresponding parameters of the ellipse criterion are $\alpha = 0.407$, $\tau_0 = 909\,\text{Mpa}$ and $\sigma_0 = 2231\,\text{Mpa}$, respectively. Accordingly, the ellipse criterion equation for the current Zr-based BMGs can be quantitatively expressed as below,

Journal of Applied Mechanics. Received August 28, 2017;
Accepted manuscript posted October 30, 2017. doi:10.1115/1.4038286

$$\frac{\sigma^2}{2231^2}+\frac{\tau^2}{909^2}=1 \quad . \tag{21}$$

The critical point which is mentioned in Eq. (20) can be given $\rho_{cr}=1-2\alpha^2=0.6654$. The calculation results for different ρ $(-1\le\rho\le\rho_{cr})$ are shown in Fig. 3.

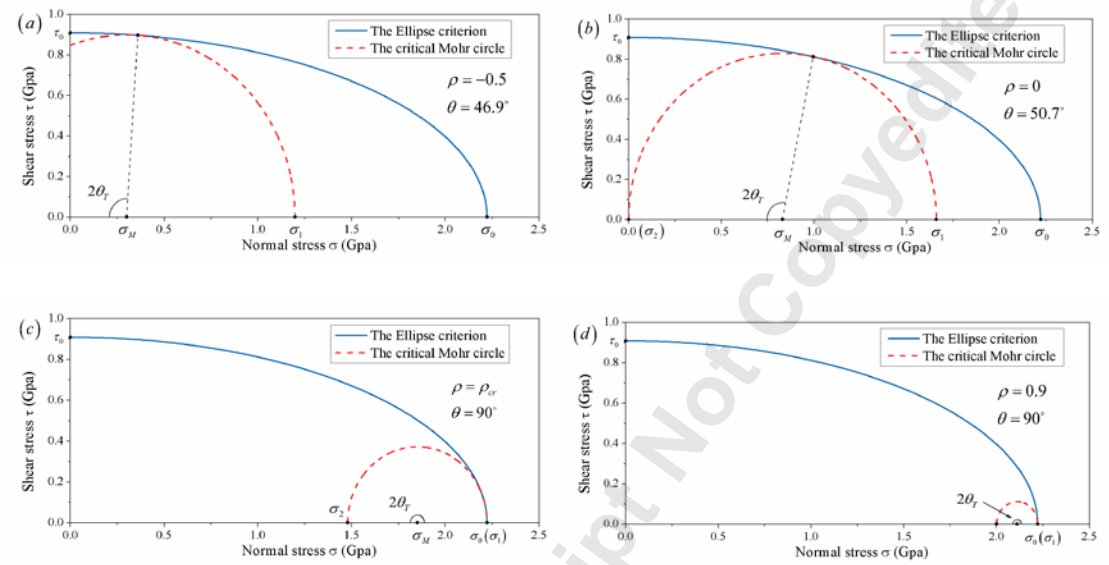

Fig. 3. The critical Mohr circles for different loading modes and the critical fracture lines of the ellipse criterion. (a) $\rho=-0.5$, (b) $\rho=0$, (c) $\rho=\rho_{cr}$, (d) $\rho=0.9$.

The critical fracture lines of the ellipse criterion and the corresponding critical Mohr circles for different ρ (from -0.5 to$1-2\alpha^2$) are plotted in the Fig. 3(a)-Fig 3(c). With ρ increasing, the critical Mohr circle moves along the positive direction of σ-axis, and the radius of the critical Mohr circle decreases. Furthermore, the tangent point moves from the vertex on the minor axis of the ellipse to that on the major axis. When $\rho=\rho_{cr}$, the shear stress of the fracture plane equals zero, and the normal stress σ_{11} equals to σ_0.

Journal of Applied Mechanics. Received August 28, 2017;
Accepted manuscript posted October 30, 2017. doi:10.1115/1.4038286

3.2 Fracture behaviors of bulk metallic glasses in the case $\rho_{cr} \le \rho < 1$

Now we discuss fracture behaviors of BMGs in the case of $\rho_{cr} \le \rho < 1$. When $\rho = \rho_{cr}$, the fracture takes place with zero shear stress on the fracture plane. When ρ takes the value from ρ_{cr} to 1, it can be speculated that the fracture will still occur on the 90° plane. This is because in this condition the normal stress on this plane will satisfy the fracture condition first no matter what σ_{22} is.

This could be demonstrated from the perspective of Mohr circle. As shown in the Fig. 3(a) to Fig 3(c), the tangent point moves to the rightmost of the ellipse with ρ increasing from -1 to ρ_{cr}. When $\rho > \rho_{cr}$, the Mohr circle is too small to contact with the ellipse until it meets the vertex on the major axis of the ellipse, and for this reason, the fracture still occurs on the 90° plane as we speculated. In the end, the Mohr circle will reduce to a point with $\rho = 1$. A typical case for ρ=0.9 is shown in Fig. 3d.

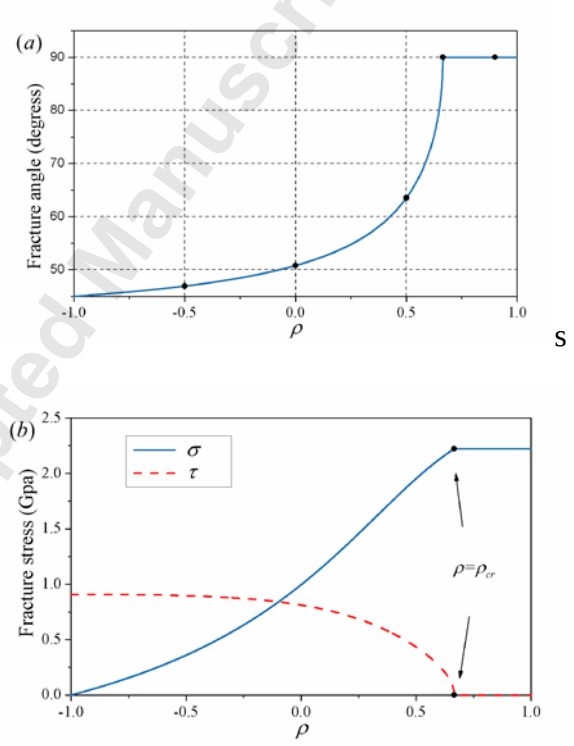

Fig. 4. The variation of fracture angle and critical stresses with respect to the proportionality coefficient ρ. (a) Variation of the fracture angle with the

proportionality coefficient ρ. The points denote the fracture angle of the loading pattern shown in the Figs. 3(a)-(d). (b) The shear stress and normal stress on the fracture plane. The points denote the results of fracture stress while $\rho=\rho_{cr}$.

With the above discussion, the variation of fracture angle and critical stresses on fracture plane with respect to the proportionality coefficient ρ is shown in Fig. 4. The fracture angle increases gradually from 45° to 90° plane with the increasing of ρ (see Fig. 4(a)), and the corresponding the critical normal and shear stress on the fracture plane are shown in Fig. 4(b). In this process, shear stress gradually decreases, while the normal stress becomes larger and dominates the fracture of BMGs. When $\rho>\rho_{cr}$ the critical shear stress on the fracture plane equals to zero suggesting that in this case only normal stress is needed to destroy the BMGs, and the fracture takes place on the 90° plane with τ=0 and $\sigma_{11}=\sigma_0$. For $\rho_{cr}\le\rho<1$, it is interesting to find that the ellipse criterion can reduce to the maximum normal stress criterion.

3.3 The new form of the ellipse criterion

Fracture criteria usually choose the normal and shear stress on the fracture plane as the basic variables. However, they can only be obtained after the fracture angle is determined. Thus, these criteria are not convenient to be applied in engineering applications.

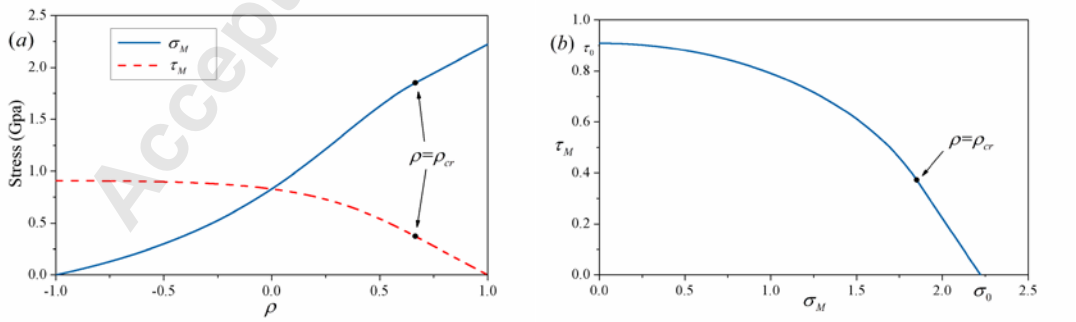

Fig. 5. Fracture behaviors of BMGs based on τ_M and σ_M. (a) Variation of σ_M and τ_M with ρ. (b) τ_M versus σ_M. The points denote the results of fracture

stress while $\rho=\rho_{cr}$.

The variation of τ_M and σ_M for different loading modes is shown in the Fig. 5. As a sister equation of Eq. (6), Eq. (19) combining with Eq. (13) makes up a new fracture criterion for BMGs, which is more convenient to be applied in engineering applications.

3.4 Comparisons between the theoretical results and the existing experiments for complex loading

The complex mechanical loading experiments for Vit 1 were well performed in Ref.[16, 20], where the cylindrical specimens were 12.7 mm in length and 6.35 ± 0.02 mm in diameter, and were subject to the quasi-static tension with superimposed pressure. There are 11 experimental points of tension provided in their papers [16,20], including a point, which is fail near collar. However, the samples tested in tension under atmospheric pressure (0.1 MPa) exhibited a fracture plane perpendicular to the tensile axis, and there is an outer fracture rim oriented at 50°-53° to the tensile axis approximately 200 μm in width on the fracture plane [20]. It may be caused by the influence of residual polishing scratches on the surface of the specimen which was mentioned in their paper [23]. To relieve the effects of residual polishing scratches, only points from the results with superimposed pressure larger than 450 MPa are selected. Besides, fracture behaviors of Vit 1 with pressure up to 1300 Mpa was carefully investigated recently [16]. The experimental data in this study are also used to compare with our theoretical analysis results except one of these points that is fail with lager pressure (in this case, the tensile normal stress becomes negative on fracture plane, which is beyond the scope of this article). Finally, seven experimental points are used to compare with our theoretical analysis results.

Since there is no data for uniaxial tension, two experimental data are selected to

obtain the intrinsic parameters α and τ_0 of Vit 1 for the ellipse criterion. To be specific, σ_A=0.7965 Gpa , τ_A=0.8601 Gpa and σ_B=0.3769 Gpa τ_B=0.9949 Gpa , are used to obtain the parameters of the ellipse criterion, which are $\alpha = 0.7257$ and $\tau_0 = 1.0363\,\text{Gpa}$. Meanwhile, the fracture lines of the M-C criterion and the ellipse are supposed to be tangent at point B, so that the coefficient for the M-C criterion can be obtained, $\mu = 0.1995$ and $\tau_0 = 1.019\,\text{Gpa}$.

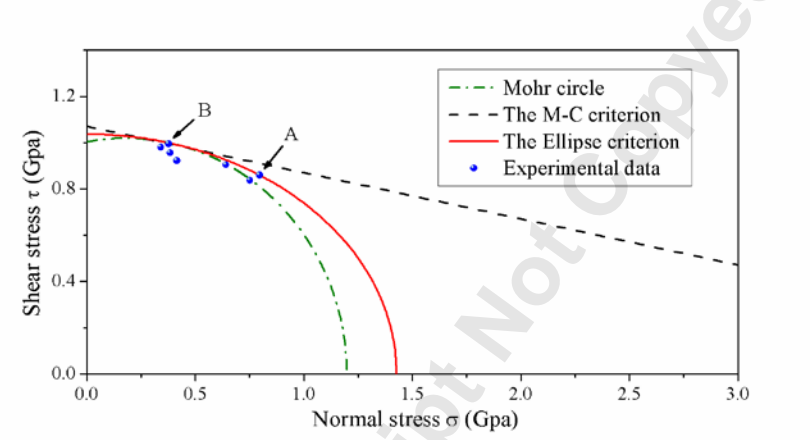

Fig. 6. Variation of the shear fracture stress with respect to the normal stress acting on the fracture plane. The critical fracture lines of the two criteria as well as the tangent point B for Mohr's circle are plotted for comparisons.

The variation of the shear fracture stress with respect to the normal stress according to our theoretical analysis is shown in Fig. 6, and the experimental data is provided for comparisons. It can be seen that our method combing with the ellipse criterion could well reproduce the experiment results.

Journal of Applied Mechanics. Received August 28, 2017;
Accepted manuscript posted October 30, 2017. doi:10.1115/1.4038286

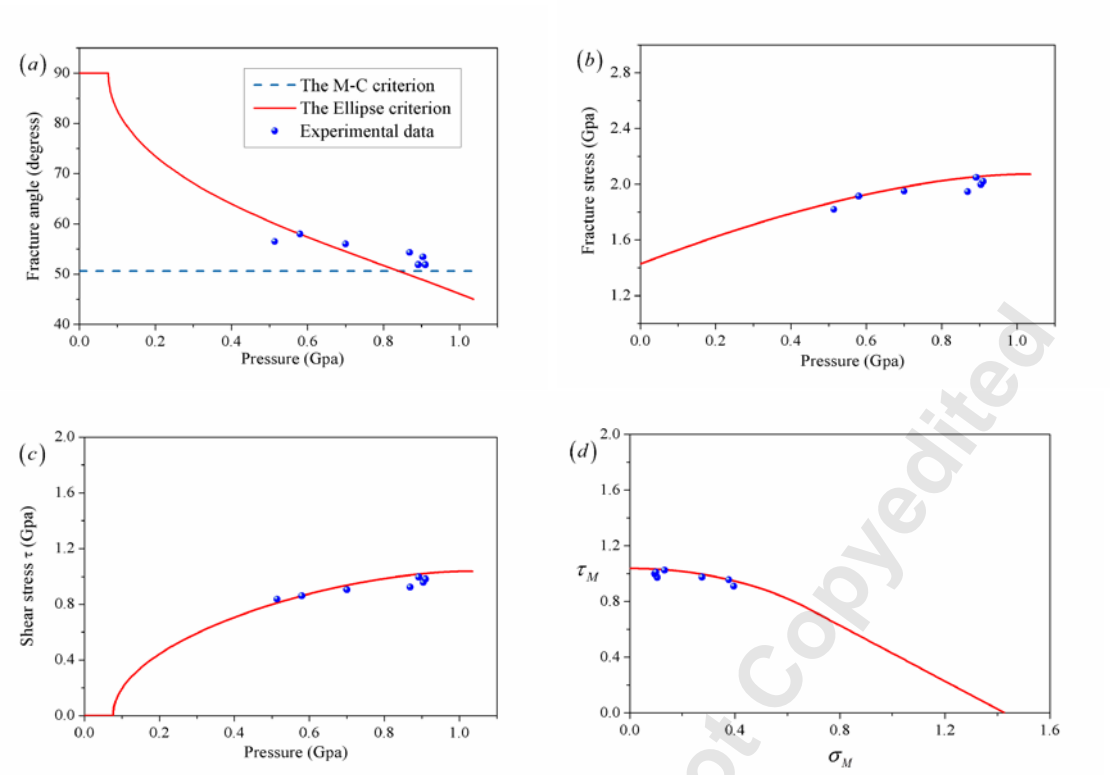

Fig. 7. **Comparisons between the theoretical calculation results and experimental points** (a) fracture angle versus confining pressure, (b) axial fracture stress σ_1 versus confining pressure, (c) shear stress on the fracture plane versus confining pressure. (d) τ_M versus σ_M.

The results shown in Fig. 6 indicate that both two criteria can be used to predict the fracture strength in experiments. However, the experimental data shown in Fig. 7(a) illustrates that the fracture angle vary with the confining pressure. As mentioned above, the M-C criterion is incapable to describe the variation of fracture angle, while our formula combining with the ellipse criterion could well predict the experimental results of fracture angle. The comparison between the theoretical analysis results and experimental data for σ_M and τ_M is shown in Fig. 7(d).

4. Conclusion

In this paper, we establish a universal formula for the fracture angle. This formula

is not limited to specific fracture criteria or loading modes. The ellipse criterion has been used as an example to show how to apply our formula to a specific case. The results show that fracture modes can be divided to three parts :(1) Pure shear mode, where $\rho = -1$ and the fracture of BMGs happens owing to the shear stress only. (2) For $-1 < \rho < \rho_{cr}$, both the critical normal stress and shear stress contribute to the fracture. With the critical tensile normal stress increasing, the critical shear stress τ will decrease, and the fracture angle changes accordingly from 45° to 90° during this process. (3) Pure tensile mode, once $\rho > \rho_{cr}$, the fracture plane is perpendicular to the x_1-axis, and only the normal stress is needed to destroy the materials suggesting that the shear stress plays no role in this situation. In this case, it is interesting to find that the ellipse criterion can reduce to the maximum normal stress criterion. Moreover, we obtain a new ellipse criterion (19) based on the mean stress σ_M and maximum shear stress τ_M, which is more convenient to be applied in engineering applications. Through comparing with experiments, it is found that the universal formula (5) for the fracture angle combining with the ellipse criterion can well reproduce the fracture angle and strength of BMGs under complex loading.

Acknowledgments

The authors thank Dr. Feng Liu for his valuable help to revise our paper. This work was financially supported by the National Natural Science Foundation of China (Grant Nos. 11602272, 11602270, 11021262, and 11532013), the National Basic Research Program of China (”973” Project) (Grant No. 2012CB937500), and the Strategic Priority Research Program of the Chinese Academy of Sciences (Grant No. XDB22040503).

Competing interests: The authors declare no competing interests.

References

[1] Klement, W., Willens, R., and Duwez, P., 1960, "Non-crystalline structure in solidified gold–silicon alloys," Nature, 187(4740), pp. 869-870.

[2] Johnson, W. L., 1986, "Thermodynamic and kinetic aspects of the crystal to glass transformation in metallic materials," Progress in Materials Science, 30(2), pp. 81-134.

[3] Greer, A. L., 1995, "Metallic glasses," Science, 267(5206), p. 1947.

[4] Inoue, A., 2000, "Stabilization of metallic supercooled liquid and bulk amorphous alloys," Acta materialia, 48(1), pp. 279-306.

[5] Schuh, C. A., Hufnagel, T. C., and Ramamurty, U., 2007, "Mechanical behavior of amorphous alloys," Acta Materialia, 55(12), pp. 4067-4109.

[6] Steif, P., Spaepen, F., and Hutchinson, J., 1982, "Strain localization in amorphous metals," Acta Metallurgica, 30(2), pp. 447-455.

[7] Chen, H., He, Y., Shiflet, G., and Poon, S., 1994, "Deformation-induced nanocrystal formation in shear bands of amorphous alloys," Nature, 367(6463), pp. 541-543.

[8] Flores, K. M., and Dauskardt, R. H., 1999, "Local heating associated with crack tip plasticity in Zr–Ti–Ni–Cu–Be bulk amorphous metals," Journal of materials research, 14(03), pp. 638-643.

[9] Hays, C., Kim, C., and Johnson, W. L., 2000, "Microstructure controlled shear band pattern formation and enhanced plasticity of bulk metallic glasses containing in situ formed ductile phase dendrite dispersions," Physical Review Letters, 84(13), p. 2901.

[10] Xing, L.-Q., Li, Y., Ramesh, K., Li, J., and Hufnagel, T., 2001, "Enhanced plastic strain in Zr-based bulk amorphous alloys," Physical Review B, 64(18), p. 180201.

[11] Donovan, P., 1988, "Compressive deformation of amorphous Pd40Ni40P20," Materials Science and Engineering, 98, pp. 487-490.

[12] Liu, C., Heatherly, L., Horton, J., Easton, D., Carmichael, C., Wright, J., Schneibel, J., Yoo, M., Chen, C., and Inoue, A., 1998, "Test environments and mechanical properties of Zr-base bulk amorphous alloys," Metallurgical and Materials Transactions A, 29(7), pp. 1811-1820.

[13] Zhang, Z., He, G., Eckert, J., and Schultz, L., 2003, "Fracture mechanisms in bulk metallic glassy materials," Physical review letters, 91(4), p. 045505.

[14] Mukai, T., Nieh, T., Kawamura, Y., Inoue, A., and Higashi, K., 2002, "Effect of strain rate on compressive behavior of a Pd 40 Ni 40 P 20 bulk metallic glass," Intermetallics, 10(11), pp. 1071-1077.

[15] Flores, K., and Dauskardt, R., 2001, "Mean stress effects on flow localization and failure in a bulk metallic glass," Acta Materialia, 49(13), pp. 2527-2537.

[16] Caris, J., and Lewandowski, J., 2010, "Pressure effects on metallic glasses," Acta Materialia, 58(3), pp. 1026-1036.

[17] Yu, M.-h., 2002, "Advances in strength theories for materials under complex stress state in the 20th century," Applied Mechanics Reviews, 55(3), pp. 169-218.

[18] Irgens, F., 2008, Continuum mechanics, Springer Science & Business Media.

[19] Zhang, Z., and Eckert, J., 2005, "Unified tensile fracture criterion," Physical review letters, 94(9), p. 094301.

[20] Lewandowski, J. J., and Lowhaphandu, P., 2002, "Effects of hydrostatic pressure on the flow and fracture of a bulk amorphous metal," Philosophical magazine A, 82(17-18), pp. 3427-3441.
[21] Chen, C., Gao, M., Wang, C., Wang, W.-H., and Wang, T.-C., 2016, "Fracture behaviors under pure shear loading in bulk metallic glasses," Scientific Reports, 6.
[22] Qu, R. T., Eckert, J., and Zhang, Z. F., 2011, "Tensile fracture criterion of metallic glass," Journal of Applied Physics, 109(8), p. 083544.
[23] Lowhaphandu, P., Montgomery, S., and Lewandowski, J. J., 1999, "Effects of superimposed hydrostatic pressure on flow and fracture of a Zr-Ti-Ni-Cu-Be bulk amorphous alloy," Scripta materialia, 41(1), pp. 19-24.